

See discussions, stats, and author profiles for this publication at: <https://www.researchgate.net/publication/244426191>

# Raman, Infrared, and Surface-Enhanced Raman Spectroscopy in Combination with ab Initio and Density Functional Theory Calculations on 10Isopropyl10 H -phenothiazine-5-oxide

ARTICLE in THE JOURNAL OF PHYSICAL CHEMISTRY A · JUNE 2003

Impact Factor: 2.69 · DOI: 10.1021/jp021731j

CITATIONS

29

READS

25

## 5 AUTHORS, INCLUDING:



**Traian Iliescu**

Babeş-Bolyai University

69 PUBLICATIONS 503 CITATIONS

SEE PROFILE



**Florin Dan Irimie**

Babeş-Bolyai University

80 PUBLICATIONS 664 CITATIONS

SEE PROFILE



**Wolfgang Kiefer**

University of Wuerzburg

881 PUBLICATIONS 9,866 CITATIONS

SEE PROFILE

# Raman, Infrared, and Surface-Enhanced Raman Spectroscopy in Combination with ab Initio and Density Functional Theory Calculations on 10-Isopropyl-10H-phenothiazine-5-oxide

M. Bolboaca,<sup>†</sup> T. Iliescu,<sup>‡</sup> Cs. Paizs,<sup>§</sup> F. D. Irimie,<sup>§</sup> and W. Kiefer<sup>\*,†</sup>

*Institut für Physikalische Chemie, Universität Würzburg, D-97074 Würzburg, Germany, Physics Department, Babes-Bolyai University, 3400 Cluj-Napoca, Romania, and Chemistry Department, Babes-Bolyai University, 3400 Cluj-Napoca, Romania*

*Received: July 25, 2002; In Final Form: December 12, 2002*

Raman, infrared, and surface-enhanced Raman spectroscopies were applied to the vibrational characterization of the most stable conformer of the 10-isopropyl-10H-phenothiazine-5-oxide derivative. To find the optimized structure and the computed vibrational wavenumbers of the title compound, ab initio calculations at the Hartree–Fock level of theory and density functional theory calculations at the BPW91 and B3LYP levels of theory were performed. The comparison of the surface-enhanced Raman (SER) spectra, obtained only on activated silver colloids, with the corresponding Raman spectra reveals small shifts ( $\Delta\nu \leq 5 \text{ cm}^{-1}$ ) and proves the partial chemisorption of the molecules on the silver surface via the lone pair electrons of the oxygen atom; the electromagnetic mechanism is the main mechanism of the enhancement. Variations of the SER spectra with the change of pH were attributed to the orientational changes of the adsorbed molecules with respect to the silver surface.

## Introduction

Phenothiazine and its derivatives have been extensively investigated because of their interesting pharmacological activity.<sup>1–3</sup> Phenothiazine and related compounds have significant physiological activity and can be used as tranquilizers.<sup>4</sup> A new series of phenothiazine derivatives, which are important intermediates in the metabolism of phenothiazine drugs, have been prepared,<sup>5,6</sup> and the schematic structure of 10-isopropyl-10H-phenothiazine-5-oxide compound is illustrated in Figure 1.

Raman spectroscopy is an invaluable tool to provide information about the structure and interacting mechanisms of biologically active molecules. The Raman spectra of phenothiazine and its radical cation were reported by Pan and Phillips,<sup>7</sup> while Hester and Williams<sup>8</sup> have reported the resonance Raman spectra of phenothiazine, 10-methylphenothiazine, and their radical cations. A number of recent studies have examined the photooxidation behavior of the phenothiazines and their radical cations, using time-resolved laser flash photolysis experiments.<sup>9–11</sup>

However, the application of the conventional Raman spectroscopy is limited by the weak intensity of the Raman scattered light and the interference of the fluorescence. One way to overcome these disadvantages is surface-enhanced Raman spectroscopy (SERS).<sup>12,13</sup> The origin of the enhancement of Raman scattering cross section at rough surfaces has been an active field of research. It is now widely accepted that there are two main contributions to the overall SERS effect: an electromagnetic contribution and a chemical effect.<sup>12,14</sup> The electromagnetic (EM) mechanism of the Raman enhancement

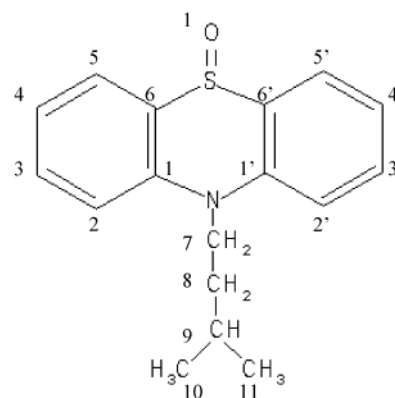


**Figure 1.** Schematic structure of 10-isopropyl-10H-phenothiazine-5-oxide compound.

is based on an increase in the electromagnetic field intensity near the metal surface due to a resonant excitation of the delocalized electrons of the metal. This effect is not dependent on the specific interactions between the molecules and the metal but is strongly related to the large-scale roughness that characterizes the substrate surface.<sup>12</sup> In the short-range chemical or charge-transfer (CT) mechanism, a modulation of the molecule's electronic polarizability arising from the interaction with the metal surface is responsible for the enhancement, and the chemical nature of the molecules becomes important.<sup>14,15</sup>

In the present paper, a rather detailed experimental and theoretical study of the most stable conformer of the 10-isopropyl-10H-phenothiazine-5-oxide compound has been carried out. The first part of the study presents vibrational analysis of the above-mentioned phenothiazine derivative from an analytical (infrared and Raman spectroscopy) and theoretical (Hartree–Fock (HF) and density functional theory (DFT) calculations) point of view, while in the second part of the study,

\* Corresponding author. Fax: +49 0931 888 6332. E-mail: wolfgang.kiefer@mail.uni-wuerzburg.de.

<sup>†</sup> Universität Würzburg.

<sup>‡</sup> Babes-Bolyai University, Physics Department.

<sup>§</sup> Babes-Bolyai University, Chemistry Department.

the SER spectra at different pH values are reported and analyzed in order to elucidate the adsorption behavior of the molecules on colloidal silver particles and to establish whether the molecule–substrate interaction and, consequently, the SERS effect may be dependent on the pH of the solution.

## Experimental Section

**Sample and Instrumentation.** All starting materials involved in substrate and sample preparation were purchased from commercial sources as analytical pure reagents.

A sodium citrate silver colloid, prepared according to the standard procedure of Lee and Meisel,<sup>16</sup> was employed as SERS substrate. AgNO<sub>3</sub> (90 mg) was dissolved in 500 mL of water and heated to boiling with continuous stirring. A 10 mL portion of 1% aqueous trisodium citrate was added dropwise, and the reaction mixture was boiled for another 60 min. The resultant colloid was yellowish gray with an absorption maximum at 407 nm. Small amounts of 10-isopropyl-10*H*-phenothiazine-5-oxide 10<sup>−1</sup> M ethanol solutions were added to 3 mL of silver colloid. NaCl solution (10<sup>−2</sup> M) was also added (10:1) for production of a stabilization of the colloidal dispersion that leads to a considerable enhancement of the SER signal.<sup>17</sup> The final concentration of the sample was ~2.5 10<sup>−4</sup> M. NaOH and HCl were used to adjust the pH values.

The UV–vis absorption spectra were recorded with a Perkin-Elmer Lambda 19 UV–vis–NIR spectrometer with a scan speed of 240 nm/min.

The FT-Raman spectrum of polycrystalline sample was recorded using a Bruker IFS 120HR spectrometer with an integrated FRA 106 Raman module and a resolution of 2 cm<sup>−1</sup>. Radiation of 1064 nm from an Nd:YAG laser was employed for excitation. A Ge detector, cooled with liquid nitrogen, was used. The infrared spectrum in KBr pellets was recorded with a Bruker IFS 25 spectrometer and a resolution of 2 cm<sup>−1</sup>. In both cases, the spectral data were analyzed using OPUS 2.0.5. software. The SER spectra of the sample on silver colloid, collected in the backscattering geometry, were recorded with a Spex 1404 double spectrometer, using 514.5 nm and 300 mW output of a Spectra Physics argon ion laser. The detection of the Raman signal was carried out with a Photometrics model 9000 CCD camera. The spectral resolution was 2 cm<sup>−1</sup>. In this case, the MAPS VO 98.5 analyzing software package was used for the acquisition of data.

**Computational Details.** Theoretical calculations of the structure and vibrational wavenumbers of the investigated compound were performed using the Gaussian 98 program package.<sup>18</sup> The DFT calculations were carried out with Becke's 1988 exchange functional<sup>19</sup> and the Perdew–Wang 91 gradient corrected correlation functional (abbreviated as BPW91)<sup>20</sup> and Becke's three-parameter hybrid method using the Lee–Yang–Parr correlation functional (abbreviated as B3LYP).<sup>21</sup> For comparison purposes, ab initio calculations performed at the HF level of theory were also done. The 6-31G\* Pople split-valence polarization basis set was used in the geometry optimization and normal modes calculations at all theoretical levels. At the optimized structure of the examined species, no imaginary frequency modes were obtained, proving that a local minimum on the potential energy surface was found.

## Results and Discussion

**Vibrational Analysis.** Due to the flexibility of the isopropyl group, the 10-isopropyl-10*H*-phenothiazine-5-oxide molecule allows for several conformers. The optimized geometries of the six most probable conformers calculated at the BPW91/6-31G\*

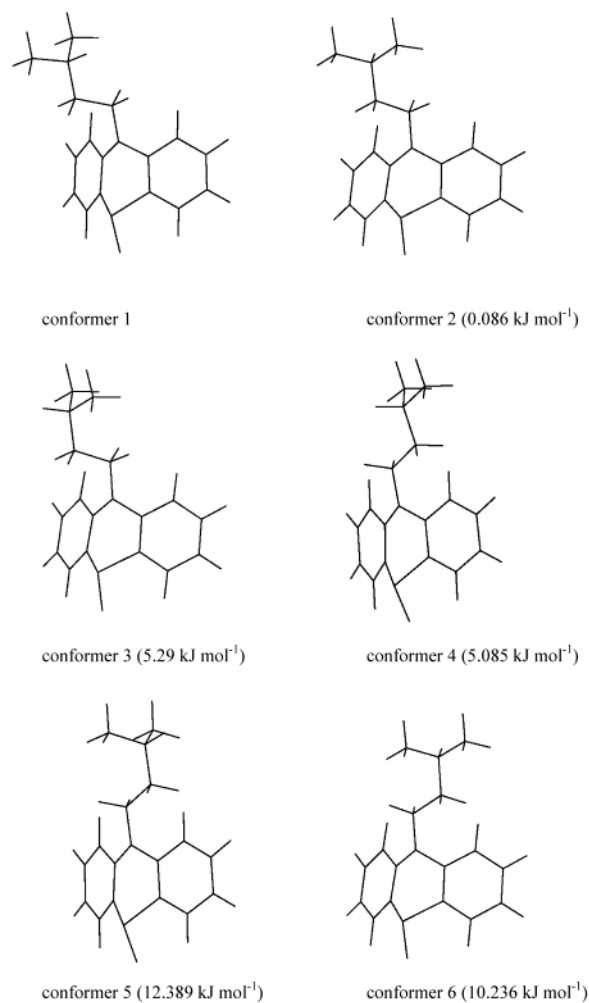


**Figure 2.** Optimized geometries of six most probable conformers of 10-isopropyl-10*H*-phenothiazine-5-oxide. The differences between the energy of the most stable conformer and the energy of the other conformers, obtained at the BPW91/6-31G\* level of theory, are indicated in parentheses.

level of theory are illustrated in Figure 2. Analytical harmonic vibrational modes have also been calculated in order to ensure that the optimized structures correspond to minima on the potential energy surface. The total energy of the most stable conformer, which was found to be conformer 1, including zero point corrections, is −1186.6367 hartree. The differences between the energy of the most stable conformer and the energy of the other relevant conformers, obtained at this theoretical level, are also indicated in Figure 2. The experimental and theoretical investigations were further carried out for conformer 1, which will be denoted as 10-isopropyl-10*H*-phenothiazine-5-oxide.

Crystallographic analysis of phenothiazine<sup>22</sup> shows that the molecule is folded about the N–S axis, with the two planes containing the phenyl rings having a dihedral angle of 158.5°. The amount of folding increases for larger substituents on 10-substituted derivatives,<sup>7</sup> with chlorpromazine having a dihedral angle of 139.4°.

Selected optimized structural parameters of 10-isopropyl-10*H*-phenothiazine-5-oxide derivative calculated by various methods are given in Table 1 along with the available X-ray values of the ground state of the phenothiazine.<sup>22</sup> As it can be observed, the theoretical dihedral angle between the two phenyl rings of the compound has smaller values compared to the dihedral angle of the phenothiazine and is in agreement with previous results.<sup>7</sup>

**TABLE 1: Selected Calculated Bond Lengths (pm) and Angles (deg) of the 10-Isopropyl-10*H*-phenothiazine-5-oxide Compound Compared to the Experimental Data of the Phenothiazine**

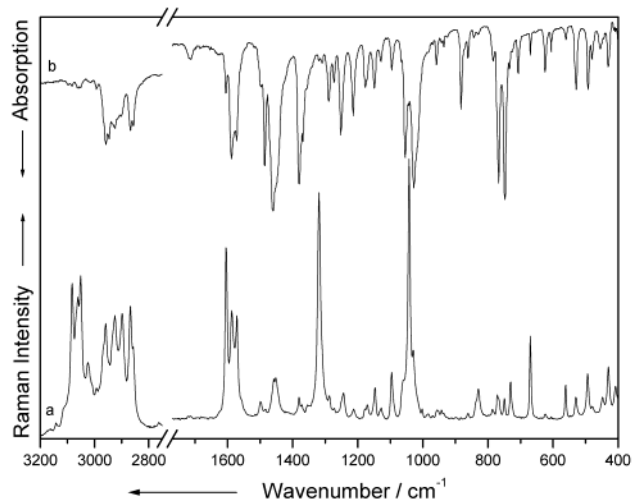
	10-isopropyl-10 <i>H</i> -phenothiazine-5-oxide			phenothiazine
	calcd <sup>a</sup>	calcd <sup>b</sup>	calcd <sup>c</sup>	exptl <sup>d</sup>
Bond lengths (pm)				
C–S <sub>avg</sub>	182.155	182.150	180.995	177
C–N <sub>avg</sub>	141.925	141.927	141.717	140.6
C <sub>1</sub> –C <sub>2</sub>	141.209	141.209	140.419	138.5
C <sub>2</sub> –C <sub>3</sub>	140.209	140.208	139.584	139
C <sub>3</sub> –C <sub>4</sub>	140.258	140.258	139.565	136.7
C <sub>4</sub> –C <sub>5</sub>	140.181	140.181	139.513	136.7
C <sub>5</sub> –C <sub>6</sub>	139.620	139.619	138.976	139.1
C <sub>6</sub> –C <sub>1</sub>	141.328	141.328	140.552	139.7
C <sub>2</sub> –H <sub>2</sub>	109.187	109.187	108.450	98
C <sub>3</sub> –H <sub>3</sub>	109.367	109.367	108.670	105
C <sub>4</sub> –H <sub>4</sub>	109.282	109.282	108.584	98
C <sub>5</sub> –H <sub>5</sub>	109.365	109.365	108.633	93
S–O <sub>1</sub>	152.295	152.295	151.280	
C <sub>7</sub> –N	147.130	147.130	146.690	
Angles (deg)				
dihedral angle	138.478	138.478	137.657	153.30
C <sub>6</sub> –S–C <sub>6</sub>	93.068	93.068	93.676	99.60
C <sub>1</sub> –N–C <sub>1</sub>	117.207	117.206	116.922	121.50
C <sub>1</sub> –C <sub>2</sub> –C <sub>3</sub>	120.484	120.484	120.417	119.8
C <sub>2</sub> –C <sub>3</sub> –C <sub>4</sub>	121.091	121.092	121.084	120.5
C <sub>3</sub> –C <sub>4</sub> –C <sub>5</sub>	119.165	119.165	119.192	119.4
C <sub>4</sub> –C <sub>5</sub> –C <sub>6</sub>	119.538	119.538	119.502	119.7
C <sub>5</sub> –C <sub>6</sub> –C <sub>1</sub>	122.307	122.307	122.268	119.2
C <sub>6</sub> –C <sub>1</sub> –C <sub>2</sub>	117.377	117.377	117.501	119.5
C <sub>1</sub> –C <sub>2</sub> –H <sub>2</sub>	120.267	120.267	120.302	118.5
C <sub>2</sub> –C <sub>3</sub> –H <sub>3</sub>	118.874	118.873	118.915	115.8
C <sub>3</sub> –C <sub>4</sub> –H <sub>4</sub>	120.554	120.554	120.520	117
C <sub>4</sub> –C <sub>5</sub> –H <sub>5</sub>	121.874	121.874	121.842	122.8
C <sub>6</sub> –S–O <sub>1</sub>	110.020	110.020	109.540	
C <sub>6</sub> –S–O <sub>1</sub>	110.065	110.650	109.567	

<sup>a</sup> RHF/6-31G\*. <sup>b</sup> BPW91/6-31G\*. <sup>c</sup> B3LYP/6-31G\*. <sup>d</sup> Reference 22.

The calculated bond lengths and bond angles agree with the reported parameters,<sup>22</sup> and the B3LYP method gave the best results. At this level of calculation, the differences observed between the theoretical and experimental values of the structural parameters that involve the S and N atoms are most probably due to the presence of the substituents.

The FT-Raman and infrared spectra of the phenothiazine derivative 10-isopropyl-10*H*-phenothiazine-5-oxide in the range from 3200 to 400 cm<sup>−1</sup> are presented in Figure 3, and the observed bands, as well as the vibrational assignment, are summarized in Table 2. The assignment of the vibrational modes was carried out with the help of the results obtained from theoretical calculations and the work of Pan and Phillips<sup>7</sup> on the phenothiazine.

Ab initio harmonic vibrational wavenumbers are typically larger than the ones observed experimentally.<sup>23</sup> A major source of this disagreement is the neglect of anharmonicity effects in the theoretical treatment. Errors arise also because of incomplete incorporation of electron correlation and the use of finite basis sets. Since Hartree–Fock calculations tend to overestimate relatively uniform vibrational wavenumbers because of improper dissociation behavior, the predicted wavenumber values have to be scaled with general scaling factors to adjust the observed experimental values.<sup>24</sup> Thus, the restricted-Hartree–Fock (RHF) calculated vibrational wavenumbers presented in Table 2 have been uniformly scaled by 0.8953 according to the work of Scott and Radom.<sup>24</sup> Even after scaling, compared to the experiment, the RHF wavenumber is overestimated in the high wave-

**Figure 3.** FT-Raman (a) and infrared (b) spectra of 10-isopropyl-10*H*-phenothiazine-5-oxide derivative.

number region but are comparable to the experimental values in the low wavenumbers region.

In agreement with previous studies,<sup>24,25</sup> the B3LYP functional tends also to overestimate the fundamental modes compared to the BPW91 method; therefore, scaling factors have to be used to obtain a considerably better agreement with the experimental data.<sup>24,25</sup> Thus, according to the work of Rauhut and Pulay,<sup>26</sup> a scaling factor of 0.963 has been uniformly applied to the B3LYP calculated wavenumber values from Table 2. The observed disagreement between the theory and experiment could be a consequence of the anharmonicity and of the general tendency of the quantum chemical methods to overestimate the force constants at the exact equilibrium geometry.<sup>26</sup> Nevertheless, as one can see from Table 2, the theoretical calculations reproduce the experimental data well and allow the assignment of the vibrational modes.

From Figure 3, one can see that the bands assigned to the phenyl vibrational modes dominate the infrared and Raman spectra of the 10-isopropyl-10*H*-phenothiazine-5-oxide derivative. Thus, the intense bands present in the high wavenumber region (3200–3000 cm<sup>−1</sup>) of both spectra were attributed to the CH stretching vibrations of the aromatic groups. In the high wavenumber region between 3000 and 2800 cm<sup>−1</sup>, the medium intense bands assigned to the CH stretching vibrations of the isopropyl group can also be observed in both spectra. The strong infrared and Raman bands between 1605 and 1571 cm<sup>−1</sup> were given by the ring-stretching vibrational modes. The strong Raman and the corresponding weak infrared bands at 1319 cm<sup>−1</sup> (calcd 1323 cm<sup>−1</sup>) were also assigned to the CC stretching vibration of the aromatic ring. The breathing vibration of the benzene rings gives strong bands at 1042 cm<sup>−1</sup> (calcd 1042 cm<sup>−1</sup>) in both spectra. The medium intense infrared and Raman bands at 882 (calcd 871 cm<sup>−1</sup>) and 670 cm<sup>−1</sup> (calcd 666 cm<sup>−1</sup>) were assigned to the in-plane ring deformation vibrations, while the bands attributed to the out-of-plane ring deformation vibrations appear at 703 (calcd 710 cm<sup>−1</sup>), 530 (calcd 514 cm<sup>−1</sup>), and 430 cm<sup>−1</sup> (calcd 440 cm<sup>−1</sup>) in the infrared and Raman spectra of the phenothiazine derivative. The bands due to the in-plane and out-of-plane CH deformation vibrations appear in both spectra around 1200 and 750 cm<sup>−1</sup>, respectively.

The S=O deformation and stretching vibrations give rise to the medium intense Raman bands at 383 (calcd 375 cm<sup>−1</sup>) and 1095 cm<sup>−1</sup> (calcd 1087 cm<sup>−1</sup>), respectively. The medium intense Raman band at 1244 cm<sup>−1</sup> and the infrared band at 1251 cm<sup>−1</sup>

**TABLE 2: Wavenumbers (in  $\text{cm}^{-1}$ ) and Assignment of the Theoretical Wavenumber Values ( $\text{cm}^{-1}$ ) to the Experimental Bands of the Phenothiazine Derivative 10-isopropyl-10*H*-phenothiazine-5-oxide<sup>a</sup>**

IR	Raman	calcd <sup>b</sup>	calcd <sup>c</sup>	calcd <sup>d</sup>	assignment
	177m	193	185	188	C <sub>1</sub> NC <sub>1'</sub> , C <sub>6</sub> SC <sub>6'</sub> twist + SO deformation
	199m	203	202	200	CCC skeletal deformation
	272m	267	275	271	CH deformation (CH <sub>3</sub> )
	308w	320	305	308	ring chair deformation
	340m	338	333	332	C <sub>1</sub> NC <sub>1'</sub> , C <sub>6</sub> SC <sub>6'</sub> twist
	383m	372	375	372	SO deformation + C <sub>10,9,11</sub> deformation
402m	408m	408	403	384	out-of-plane Ph ring deformation
430m	430m	438	440	419	out-of-plane Ph ring deformation
455sh	448sh	461	455	438	C <sub>7,8,9</sub> deformation + CH deformation (CH <sub>3</sub> )
479m	480sh	497	490	453	C <sub>1</sub> NC <sub>1'</sub> , C <sub>6</sub> SC <sub>6'</sub> wagging
492m	494m	518	508	488	
527m	530w	522	514	509	out-of-plane Ph ring deformation
560w	560m	566	553	514	ring chair deformation
604w	605vw	606	608	586	
624m	623vw	663	658	604	in-plane Ph ring deformation
668w	670m	685	666	656	
705m	703vw	733	710	667	out-of-plane Ph ring deformation
734sh	730m	752	736	726	CH wagging (ring)
747s	749w	768	749	740	
767s	771w	776	765	749	CH deformation (CH <sub>2</sub> )
829vw	830m	804	823	811	C <sub>10,9,11</sub> stretching + CH twist (ring)
844vw	835sh	859	830	841	
881m	882vw	884	871	862	C <sub>3,4,5</sub> , C <sub>3',4',5'</sub> bending
910sh	900vw	916	904	884	CH twist (ring)
941sh	943vw	936	939	912	
959vw	956vw	963	949	945	CH deformation (CH <sub>3</sub> )
983sh	984vw	970	974	964	
1003sh	1002vw	1003	1012	1003	C <sub>1,2,3</sub> + C <sub>3,4,5</sub> bending
1027s	1030sh	1015	1031	1018	C <sub>7,8</sub> stretching
1042sh	1042s	1021	1042	1027	Ph ring breathing
1053s	1059sh	1041	1059	1041	CH bending (ring) + C <sub>6</sub> SC <sub>6'</sub> stretching + NC <sub>7</sub> stretching
1095m	1095m	1092	1087	1074	SO stretching
1128w	1127w	1114	1124	1111	CH deformation (CH <sub>2</sub> , CH <sub>3</sub> ) + C <sub>10,9,8</sub> stretching
1150m	1142m	1146	1145	1136	
1172sh	1170w	1188	1170	1154	CH bending (ring) + CH deformation (CH, CH <sub>3</sub> )
1176m	1177sh	1199	1173	1161	
1214m	1212w	1211	1213	1201	C <sub>1</sub> NC <sub>1'</sub> as. stretching + CH bending (ring))
1251m	1244m	1249	1247	1235	C <sub>1</sub> NC <sub>1'</sub> s. stretching + CH rocking (ring)
1273m	1272vw	1276	1272	1265	CH deformation (CH <sub>2</sub> ) + CH rocking (ring) + NC <sub>7</sub> stretching
1289m	1288sh	1281	1278	1269	
1319vw	1319s	1325	1323	1300	CCC stretching (Ph ring)
1359sh	1355sh	1345	1349	1319	CH deformation (CH <sub>2</sub> , CH <sub>3</sub> )
1368sh	1372sh	1366	1365	1349	
1381s	1380w	1396	1384	1378	
1449sh	1451m	1458	1455	1443	C <sub>6,1</sub> , C <sub>6',1'</sub> stretching
1460s	1457m	1467	1480	1465	
1484s	1484vw	1477	1486	1472	CH deformation (CH <sub>2</sub> , CH <sub>3</sub> )
1498sh	1498w	1496	1502	1485	
1572m	1571m	1586	1573	1561	Ph ring stretching
1588s	1587m	1600	1591	1577	
1605m	1605s	1615	1612	1596	
2868m	2867m	2882	2935	2892	CH stretching (CH, CH <sub>2</sub> , CH <sub>3</sub> )
2901sh	2898m	2921	2997	2925	
2925m	2925m	2951	3059	2938	
2958m	2958m	3013	3069	2973	
3016vw	3025m	3030	3086	2986	CH stretching (ring)
3051vw	3050s	3042	3121	2996	
3084vw	3082s	3048	3143	3071	

<sup>a</sup> Abbreviations: Ph = phenyl, w = weak, m = medium, s = strong, sh = shoulder. <sup>b</sup> Calculated with: RHF/6-31G\*. <sup>c</sup> Calculated with: BPW91/6-31G\*. <sup>d</sup> Calculated with: B3LYP/6-31G\*.

(calcd 1247  $\text{cm}^{-1}$ ) were attributed to the CNC symmetric stretching vibration, while the weak Raman band at 1212  $\text{cm}^{-1}$  and the medium intense infrared band at 1214  $\text{cm}^{-1}$  (calcd 1213  $\text{cm}^{-1}$ ) were assigned to the CNC asymmetric stretching vibration. The bands assigned to the CSC stretching vibration are present around 1055  $\text{cm}^{-1}$  (calcd 1059  $\text{cm}^{-1}$ ) in the infrared and Raman spectra of the compound. The ring chair deformation vibrations give rise to the medium intense infrared and Raman bands at 560  $\text{cm}^{-1}$  (calcd 553  $\text{cm}^{-1}$ ) and the weak Raman band

at 308  $\text{cm}^{-1}$  (calcd 305  $\text{cm}^{-1}$ ). Other bands given by the CNC and CSC out-of-plane deformation vibrations appear around 490, 340, and 177  $\text{cm}^{-1}$ , respectively.

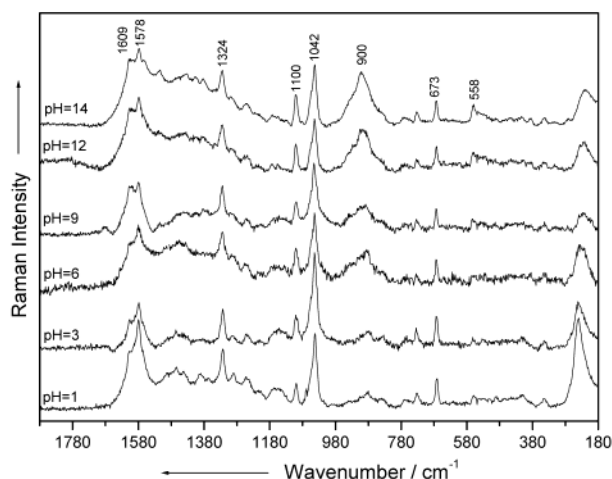
**Surface-Enhanced Raman Spectroscopy.** SER spectra of 10-isopropyl-10*H*-phenothiazine-5-oxide at different pH values have been obtained only on activated silver colloids by the presence of coadsorbed chloride anions and are presented in Figure 4. The SERS activation of the colloids in the presence of chloride anions can be explained in terms of increased



**TABLE 3: Wavenumbers (in  $\text{cm}^{-1}$ ) and Assignment of the Normal Vibrational Modes of the 10-Isopropyl-10H-phenothiazine-5-oxide Compound to the SERS Bands at Different pH Values<sup>a</sup>**

Raman	SERS			assignment
	pH 1	pH 6	pH 14	
199m	200sh 217sh 238s	203sh 218sh 238s	200sh 221ms 238sh	CCC skeletal deformation Ag–O stretching + Ag–Cl <sup>−</sup> stretching
272m	266sh	264sh	269sh	CH deformation ( $\text{CH}_3$ )
340m	347w	345w	342w	$\text{C}_1\text{NC}_{1'}$ , $\text{C}_6\text{SC}_{6'}$ twist
383m	354w	384w	388s	SO deformation + $\text{C}_{10,9,11}$ deformation
408m	408w	408vw	413w	out-of-plane Ph ring deformation
560m	558w	558m	558m	ring chair deformation
670m	671m	673m	673m	in-plane Ph ring deformation
730m	732m	734w	732m	CH wagging (Ph ring)
771w	768m	763w	769w	CH deformation ( $\text{CH}_2$ )
830m	839m	834m	833sh	$\text{C}_{10,9,8}$ stretching + CH twist (Ph ring)
882vw	880m	880m	881sh	$\text{C}_{3,4,5}$ , $\text{C}_{3',4',5'}$ bending
900vw	905sh	899m	900s	CH twist (Ph ring)
943w	936w	936sh	934sh	
1042s	1042s	1042s	1042s	Ph ring breathing
1059sh	1067m	1066sh		CH bending (Ph ring) + $\text{C}_6\text{SC}_{6'}$ stretching + $\text{NC}_7$ stretching
1095m	1098m	1100m	1100ms	SO stretching
1127w	1130sh	1136m	1133sh	CH deformation ( $\text{CH}_2$ , $\text{CH}_3$ ) + $\text{C}_{10,9,8}$ stretching
1142m	1153m	1151m	1155m	
1170w	1167m	1167m	1170m	CH bending (Ph ring) + CH deformation (CH, $\text{CH}_3$ )
1177sh		1175m		
1212w	1213m	1216w	1212vw	$\text{C}_1\text{NC}_{1'}$ as. stretching + CH bending (Ph ring)
1244m	1252m	1256m	1252m	$\text{C}_1\text{NC}_{1'}$ s. stretching + CH rocking (Ph ring)
1288sh	1290m	1296m	1298m	CH deformation ( $\text{CH}_2$ ) + CH rocking (Ph ring) + $\text{NC}_7$ stretching
1319s	1322s	1324s	1324s	CCC stretching (Ph ring)
1380w	1381sh	1383w	1383m	CH deformation ( $\text{CH}_2$ , $\text{CH}_3$ )
1451m	1441m	1435m	1432m	$\text{C}_{6,1}$ , $\text{C}_{6',1'}$ stretching
1457m	1462m	1456m	1456w	
1498w	1493sh	1501sh	1513m	CH deformation ( $\text{CH}_2$ , $\text{CH}_3$ )
1571m	1566sh	1566sh	1563sh	Ph ring stretching
1587m	1579s	1579s	1578s	
1605s	1607sh	1610sh	1609sh	
2867m	2868ms	2873m	2874m	CH stretching (CH, $\text{CH}_2$ , $\text{CH}_3$ )
2898m	2890sh	2898sh	2896sh	
2925m	2935m	2937ms	2936ms	
2958m	2962sh	2959sh	2963sh	
3050s	3063m	3063m	3068m	CH stretching (Ph ring)
3082s	3075sh	3085sh	3081sh	

<sup>a</sup> Abbreviations: Ph = phenyl, w = weak, m = medium, s = strong, sh = shoulder.

**Figure 4.** SERS spectra of 10-isopropyl-10H-phenothiazine-5-oxide compound on silver colloid at different pH values, as indicated.

electromagnetic field or on the basis of chemical enhancement mechanism.<sup>27</sup> The assignment of the normal vibrational modes of the phenothiazine derivative to the SERS bands at different pH values is summarized in Table 3. From the comparison between the Raman spectrum of the polycrystalline sample with the SER spectra (Figures 3a and 4), we found a good correlation

between the SERS and the Raman bands, with the wavenumber shifts of the SERS bands relative to the corresponding Raman bands never exceeding  $5 \text{ cm}^{-1}$ .

When a molecule binds to a metal surface, it can be either physisorbed or chemisorbed. In the case of physisorption,<sup>12</sup> the spectra of physisorbed and free molecules are similar. On the other hand, when the molecules are chemisorbed on the metal surface,<sup>14,15</sup> the position and the relative intensities of the SERS bands are dramatically changed, due to the overlapping of the molecular and metal orbitals that leads to the formation of a new metal–molecule SERS complex. Both the EM mechanism and the CT effect contribute to the overall SERS effect. In the case of physisorbed molecules, the electromagnetic mechanism is the main mechanism of the Raman enhancement, while in the case of chemisorption, the chemical effect is the dominant mechanism.

The phenothiazine derivative 10-isopropyl-10H-phenothiazine-5-oxide may bind to the silver surface either via the  $\pi$  orbitals of the aromatic rings or via the lone pair electrons of the nitrogen or oxygen atoms. For aromatic molecules, it is known<sup>28</sup> that the bands due to the ring vibrations are red shifted by more than  $10 \text{ cm}^{-1}$  and their bandwidths increase substantially when the molecules adsorb on the metal surface via their  $\pi$  systems. Since our SER spectra exhibit only small shifts by  $5 \text{ cm}^{-1}$  compared to the normal Raman spectrum and the

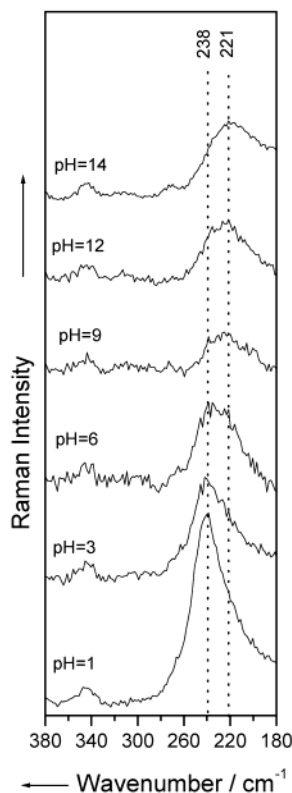


**Figure 5.** pH dependence of the metal-adsorbate stretching mode from the SER spectra of the 10-isopropyl-10*H*-phenothiazine-5-oxide compound.

bandwidths were hardly affected by the adsorption, it is likely that the molecules are adsorbed on the silver surface via the nonbonding electrons of the nitrogen or oxygen atoms. When looking at the presence of the isopropyl substituent on the nitrogen atom, we assume that the molecule-surface interaction occurs through the lone pair electrons of the oxygen atom, with the nitrogen-metal interaction being sterically hindered.

The adsorbate-metal interaction is further evidenced by the presence of some bands in the 250–150  $\text{cm}^{-1}$  region (Figure 5), which are assigned to the Ag-adsorbate stretching vibrations.<sup>29,30</sup> When the pair of the bands present in this spectral range passes from acidic to alkaline pH values, it shows intensity reversal. Thus, the intensity of the sharp band observed at pH = 1 at 238  $\text{cm}^{-1}$ , which is most probably due to the Ag-Cl<sup>-</sup> stretching vibration,<sup>29</sup> is decreased upon an increase in the pH values; meanwhile, an increase and a small shift to higher wavenumbers of the shoulder observed at 217  $\text{cm}^{-1}$  at pH = 1 occurs, which corresponds to the Ag-O stretching vibration.<sup>30</sup> The high intensity of the band at 238  $\text{cm}^{-1}$  could be explained by the increase of the chloride anions concentration in acidic environment caused by the addition of the acid for pH value adjustment. At pH = 6, the Ag-Cl<sup>-</sup> stretching band becomes broader and less intense, while the intensity of the Ag-O stretching band increases. At still higher pH (pH = 14), as the concentration of the chloride ions is reduced in the medium and, consequently, at the silver surface, the Ag-Cl<sup>-</sup> stretching vibration gives rise only to a shoulder at 238  $\text{cm}^{-1}$ , while the intensity of the band at 221  $\text{cm}^{-1}$ , which gives evidence of the metal-oxygen interaction, further increases. The appearance of the Ag-O stretching band in the SER spectra at all pH values indicates the partial chemisorption of the molecules on the metal surface through the nonbonding electrons of the oxygen atom.

The UV-vis absorption spectra of the pure colloid and mixture of the colloid and 10-isopropyl-10*H*-phenothiazine-5-

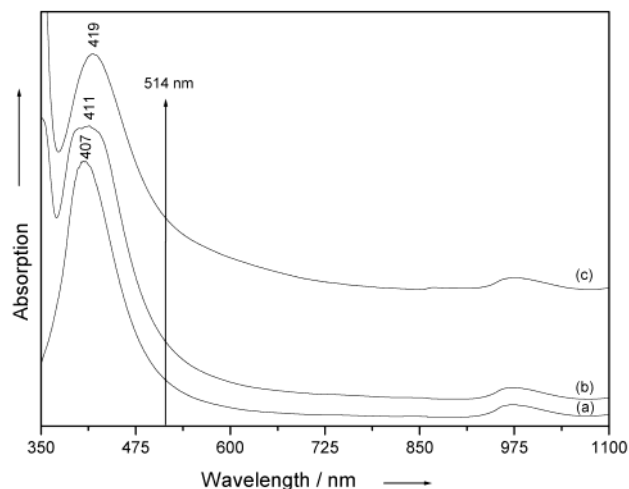


**Figure 6.** Absorption spectra of salt-free silver colloidal dispersion (a), with  $10^{-1}$  M 10-isopropyl-10*H*-phenothiazine-5-oxide (b), with  $10^{-1}$  M 10-isopropyl-10*H*-phenothiazine-5-oxide and  $10^{-2}$  M NaCl (c).

oxide before and after addition of NaCl were recorded and are presented in Figure 6. The absorption spectrum of the silver colloid shows a single absorption maximum at 407 nm, due to the small particle plasma resonance. It is known<sup>31</sup> that, when two metallic spheres approach each other, this band remains at the original single sphere wavelength, while another resonance develops at longer wavelengths; hence, a secondary peak occurs in the red/near-infrared (500–800 nm) spectral region. The appearance of such a new broad band in the red/infrared region is generally attributed to the coagulation of silver particles in the sol in the presence of the adsorbed molecules.<sup>32,33</sup> Alternatively, such a band has been ascribed to a CT band, due to the molecule-metal interaction.<sup>34</sup> One can see from Figure 6 that, after addition of sample in silver hydrosol, the band at 407 nm becomes weaker and broader and is shifted to longer wavelengths by 4 nm. When NaCl is added to the colloid-sample mixture, the absorption peak is further shifted to longer wavelengths by 8 nm, and its intensity decreases, while no new band due to the secondary plasmon resonance is observed. This behavior indicates the significant contribution of the EM mechanism to the overall SERS enhancement.

Variations in the SER spectra with the change of the pH values were usually attributed either to a change in orientation of adsorbates with respect to the metal surface<sup>35</sup> or to a change in the chemical nature of the adsorbates.<sup>36,37</sup> When the SER spectra of the phenothiazine derivative at different pH values are compared (Figure 4), as no new band appears to suggest structural changes of the molecule, the spectral changes may be attributed to an orientational change of the molecule on the silver surface.

The orientation of the adsorbed molecules with respect to the metal surface can be estimated from the enhancement of the relevant Raman bands, following the surface selection rules. According to the electromagnetic surface selection rules,<sup>38,39</sup> a vibrational mode with its normal mode component perpendicular to the metal surface is likely to become more enhanced than the parallel one. In particular, the CH stretching vibrations were reported to be relatively unambiguous probes for adsorbate orientation.<sup>40</sup>

When looking at the geometry of the 10-isopropyl-10*H*-phenothiazine-5-oxide derivative, it is very difficult to exactly predict the orientation of the molecule with respect to the metal surface. However, from Figures 4 and 3a, one may notice that, at all pH values, the bands around 1600 and 1042  $\text{cm}^{-1}$  assigned

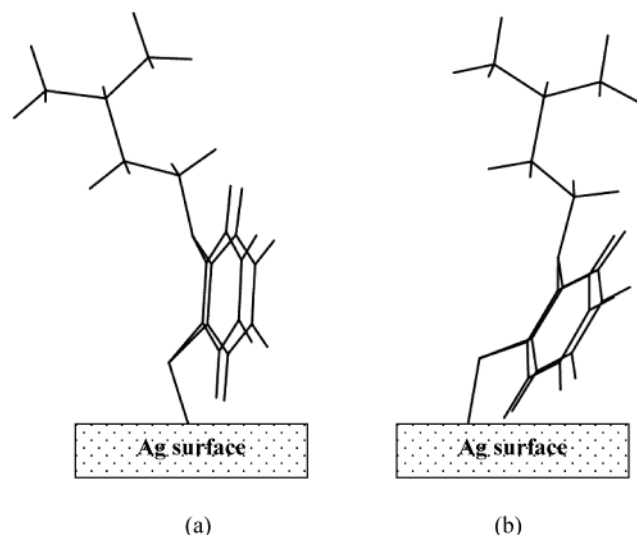


**Figure 7.** Schematic model for the adsorption geometry of 10-isopropyl-10*H*-phenothiazine-5-oxide on a colloidal silver surface at acidic (a) and alkaline (b) pH.

to the ring stretching and breathing modes, respectively, are enhanced, small shifts of the bands, due to the ring stretching vibrations compared to the corresponding Raman bands are observed (Table 3). The enhancement of the band around 670  $\text{cm}^{-1}$  given by the in-plane deformation vibration of the aromatic ring can be observed at all pH values. At alkaline pH, this band is shifted to higher wavenumbers by 3  $\text{cm}^{-1}$  compared to the Raman spectrum (Table 3). At all pH values, the bands at 408, 430, 530, and 703  $\text{cm}^{-1}$ , which arise from the out-of-plane deformation vibrations of the phenyl rings, are very weakly enhanced. The behavior of the above-mentioned bands confirms the supposition that the molecule-metal interactions do not occur via the  $\pi$  orbitals of the aromatic rings. Moreover, the enhancement and the shift to higher wavenumbers by 5  $\text{cm}^{-1}$  of the band at 1095  $\text{cm}^{-1}$  due to the SO stretching vibration (Table 3) gives further evidence of the existence of the molecule-surface interaction through the lone pair electrons of the oxygen atom. The enhancement of the bands due to the CH deformation and stretching vibrations of the isopropyl substituent present in all SER spectra confirms the major contribution of the electromagnetic effect to the SERS enhancement compared to the chemical one.

When the SER spectra at acidic and alkaline pH are compared to the normal Raman spectrum (Figures 4 and 3a), changes in the relative intensities on some bands can be noticed. Thus, at pH = 1 some bands due to the in-plane CH deformation vibration of the phenyl rings are enhanced. Furthermore, the enhancement of the bands at 1441 and 1462  $\text{cm}^{-1}$ , given by the stretching vibrations of the  $\text{C}_6\text{C}_1$  and  $\text{C}_6'\text{C}_1'$  bonds, can be explained on the basis of surface selection rules.<sup>38,39</sup> When the molecule interacts with the silver surface and adopts an upright orientation of the phenyl groups, these bonds are exactly perpendicular to the surface. For such a case, the surface selection rules predict particularly large enhancement, which is in agreement with our results. In the high wavenumber region (3200–3000  $\text{cm}^{-1}$ ), one can see the strong intensity of the CH stretching bands. Therefore, we assume that, at acidic pH, the molecules are oriented at the metal surface in such a way that the benzene rings are preponderantly perpendicular with respect to the surface as indicated in Figure 7a. According to the surface selection rules,<sup>38,39</sup> the out-of-plane vibrations are expected in the SER spectrum only when the adsorbed molecules adopt a

flat, or at least tilted, orientation on the silver surface. The increased intensity of the bands around 900  $\text{cm}^{-1}$ , attributed to the out-of-plane CH deformation vibrations of the phenyl at alkaline pH, can be a consequence of the reorientation of the aromatic rings from the upright to tilted. In contrast to the behavior revealed at acidic pH, the bands assigned to the  $\text{C}_6\text{C}_1$  and  $\text{C}_6'\text{C}_1'$  stretching vibrations are only weakly enhanced at these values of the pH. Furthermore, the intensity of the CH stretching bands present in the high wavenumber region decreases. An enhancement of the band at 558  $\text{cm}^{-1}$ , due to the ring chair deformation, is also observed. Therefore, we suppose that, at alkaline pH, a reorientation of the molecules occurs, with the phenyl rings obtaining a tilted orientation with respect to the metal surface, as suggested in Figure 7b.

## Conclusions

Experimental (infrared and Raman spectroscopy) and theoretical (HF and DFT calculations) investigations on the most stable conformer of 10-isopropyl-10*H*-phenothiazine-5-oxide derivative have been performed. The SER spectra of the sample in activated silver colloids at different pH values were recorded and compared to the normal Raman spectrum. When the shifts of the SERS bands ( $\Delta\nu \leq 5 \text{ cm}^{-1}$ ) compared to the corresponding Raman bands and the presence of the band given by the metal-molecule stretching vibration at all pH values prove the partial chemisorption of the molecules on the silver surface via the nonbonding electrons of the oxygen atom. The significant contribution of the electromagnetic mechanism to the overall SERS enhancement has been confirmed by the lack of a broad band in the long wavelength region of the absorption spectra of the colloid with added adsorbate. The changes evidenced in the SER spectra at different pH values were attributed to the reorientation of the adsorbed molecules with respect to the silver surface.

**Acknowledgment.** M.B. and W.K. acknowledge financial support from the Deutsche Forschungsgemeinschaft as well as from the Fonds der Chemischen Industrie.

## References and Notes

- (1) Shine, H. J.; Mach, E. E. *J. Org. Chem.* **1965**, *30*, 2130.
- (2) Henry, B. R.; Kasha, M. J. *J. Chem. Phys.* **1967**, *47*, 3319.
- (3) Alkalis, S. A.; Beck, G.; Grätzel, M. *J. Am. Chem. Soc.* **1975**, *97*, 5723.
- (4) Delay, J.; Deniker, P.; Harl, J. M. *Am. Med. Psychol.* **1952**, *2*, 111.
- (5) Tosa, M.; Paizs, Cs.; Majdik, C.; Poppe, L.; Kolonits, P.; Silberg, I. A.; Novak, L.; Irimie, F. D. *Heterocycl. Commun.* **2001**, *7*, 277.
- (6) Chetty, M.; Pillay, V. L.; Moodley, S. V.; Miller, R. *Eur. Neurosopharmacol.* **1996**, *6*, 85.
- (7) Pan, D.; Phillips, D. J. *J. Phys. Chem.* **1999**, *A 103*, 4737.
- (8) Hester, R.; Williams, K. P. *J. Chem. Soc., Perkin Trans.* **1981**, *2*, 852.
- (9) Guo, Q. X.; Liang, Z. X.; Liu, B.; Yao, S. D.; Liu, Y. C. *J. Photochem. Photobiol.* **1996**, *A 93*, 27.
- (10) Garcia, C.; Smith, G. A.; McGimpsey, W. M.; Kochevar, I. E.; Redmond, R. W. *J. Am. Chem. Soc.* **1995**, *117*, 10871.
- (11) Nath, S.; Pal, H.; Palit, D. K.; Sapre, A. V.; Mittal, J. P. *J. Phys. Chem.* **1998**, *A 102*, 5822.
- (12) Moskovits, M. *Rev. Mod. Phys.* **1985**, *57*, 783.
- (13) Campion, A.; Kambhampati, P. *Chem. Soc. Rev.* **1998**, *27*, 241.
- (14) Lombardi, J. R.; Birke, R. L.; Lu, T.; Xu, J. *J. Chem. Phys.* **1986**, *84*, 4174.
- (15) Creighton, J. A. *Surf. Sci.* **1983**, *124*, 209.
- (16) Lee, P. C.; Meisel, D. *J. Phys. Chem.* **1992**, *86*, 539.
- (17) Brandt, S. E.; Cotton, T. M. In *Physical Methods of Chemistry Series*, 2nd ed.; J. Wiley: New York, 1993.
- (18) Frisch, M. J.; Trucks, G. W.; Schlegel, H. B.; Scuseria, G. E.; Robb, M. A.; Cheeseman, J. R.; Zakrzewski, V. G.; Montgomery, J. A., Jr.; Stratmann, R. E.; Burant, J. C.; Dapprich, S.; Millam, J. M.; Daniels, A. D.; Kudin, K. N.; Strain, M. C.; Farkas, O.; Tomasi, J.; Barone, V.; Cossi, M.; Cammi, R.; Mennucci, B.; Pomelli, C.; Adamo, C.; Clifford, S.;



- Ochterski, J.; Petersson, G. A.; Ayala, P. Y.; Cui, Q.; Morokuma, K.; Malick, D. K.; Rabuck, A. D.; Raghavachari, K.; Foresman, J. B.; Cioslowski, J.; Ortiz, J. V.; Stefanov, B. B.; Liu, G.; Liashenko, A.; Piskorz, P.; Komaromi, I.; Gomperts, R.; Martin, R. L.; Fox, D. J.; Keith, T.; Al-Laham, M. A.; Peng, C. Y.; Nanayakkara, A.; Gonzalez, C.; Challacombe, M.; Gill, P. M. W.; Johnson, B. G.; Chen, W.; Wong, M. W.; Andres, J. L.; Head-Gordon, M.; Replogle, E. S.; Pople, J. A. *Gaussian* 98, revision A.7; Gaussian, Inc.: Pittsburgh, PA, 1998.
- (19) Becke, A. D. *Phys. Rev.* **1988**, A38, 3098.
- (20) Perdew, J. P.; Wang, Y. *Phys. Rev.* **1992**, B45, 13244.
- (21) Becke, A. D. *J. Chem. Phys.* **1993**, 98, 1372.
- (22) McDowell, J. J. H. *Acta Crystallogr.* **1976**, B32, 5.
- (23) Hehre, W. J.; Random, L.; Schleyer, P. V. R.; Pople, J. A. In *Ab Initio Molecular Orbital Theory*, J.; Wiley: New York, 1986.
- (24) Scott, A. P.; Radom, L. *J. Phys. Chem.* **1996**, 100, 16502.
- (25) Wong, M. W. *Chem. Phys. Lett.* **1996**, 256, 391.
- (26) Rauhut, G.; Pulay, P. *J. Phys. Chem.* **1995**, 99, 3093.
- (27) Hildebrandt, P.; Keller, S.; Hoffmann, A.; Vanhecke, F.; Schrader, B. *J. Raman Spectrosc.* **1993**, 24, 791.
- (28) Gao, P.; Weaver, M. J. *J. Phys. Chem.* **1985**, 89, 5040.
- (29) Sanchez-Cortes, S.; Garcia-Ramos, J. V. *J. Raman Spectrosc.* **1992**, 23, 61.
- (30) Chowdhury, J.; Ghosh, M.; Misra, T. N. *J. Colloid Interface Sci.* **2000**, 228, 372.
- (31) Muniz-Miranda, M. *Vib. Spectros.* **1999**, 19, 227.
- (32) Fu, S.; Zhang, P. *J. Raman Spectrosc.* **1992**, 23, 93.
- (33) Liang, E. J.; Engert, C.; Kiefer, W. *J. Raman Spectrosc.* **1993**, 24, 775.
- (34) Sanchez-Cortes, S.; Garcia-Ramos, J. V.; Morcillo, G.; Tinti, A. *J. Colloid Interface Sci.* **1995**, 175, 358.
- (35) Takahashi, M.; Furukawa, H.; Fujita, M.; Ito, M. *J. Phys. Chem.* **1987**, 91, 5940.
- (36) Sun, S. C.; Bernard, I.; Birke, R. L.; Lombardi, J. R. *J. Electroanal. Chem.* **1985**, 196, 359.
- (37) Anderson, M. R.; Evans, D. H. *J. Am. Chem. Soc.* **1988**, 110, 6612.
- (38) Hallmark, V. M.; Campion, A. *J. Chem. Phys.* **1986**, 84, 2933.
- (39) Moskovits, M.; Suh, J. S. *J. Phys. Chem.* **1984**, 88, 5526.
- (40) Gao, X.; Davies, J. P.; Weaver, M. J. *J. Chem. Phys.* **1990**, 94, 6858.